Numerical simulations of concrete processing: From standard formative casting to additive manufacturing

Roussel, Nicolas; Spangenberg, Jon; Wallevik, Jon; Wolfs, Rob

Published in:
Cement and Concrete Research

Link to article, DOI:
10.1016/j.cemconres.2020.106075

Publication date:
2020

Document Version
Peer reviewed version

Numerical simulations of concrete processing: From standard formative casting to additive manufacturing

Article *in* Cement and Concrete Research · September 2020

DOI: 10.1016/j.cemconres.2020.106075

CITATIONS
13

READS
758

4 authors:

N. Roussel
Université Gustave Eiffel
183 PUBLICATIONS **9,633** CITATIONS
SEE PROFILE

Jon Spangenberg
Technical University of Denmark
65 PUBLICATIONS **693** CITATIONS
SEE PROFILE

Jon Elvar Wallevik
Icelandic Meteorological Office
33 PUBLICATIONS **1,524** CITATIONS
SEE PROFILE

Rob Wolfs
Eindhoven University of Technology
27 PUBLICATIONS **1,291** CITATIONS
SEE PROFILE

Please cite this paper as Cem. Concr. Res. 135 (2020) 106075
https://doi.org/10.1016/j.cemconres.2020.106075
Corresponding author: nicolas.roussel@ifsttar.fr

Numerical simulations of concrete processing: from standard formative casting to additive manufacturing

Nicolas Roussel, Jon Spangenberg, Jon Wallevik, Rob Wolfs

Abstract

The concrete industry is facing new digital shaping processes that still have to be optimized and that require cement-based materials, for which fresh properties requirements are yet to be defined. In this paper, we first present the state of the art in the field of numerical simulations of concrete flow. We then focus on the literature on numerical simulations of extrusion-based additive manufacturing processes for concrete. Our review shows that the available numerical modeling tools are able to detect and predict various types type of failures through the printing process, no matter if these happen at the scale of the nozzle, of one printed layer or of the entire object being printed. As they allow for a systematic evaluation of the influence of the entire range of material, geometric and process parameters, numerical modeling is a valid option to optimize both process and material.

1. *Introduction*

Shaping is a complex process. Most shapes in nature or industry result from the competition between forces and/or energies. This also applies to concrete shaping in the construction industry where shaping is traditionally a formative process, in which the competition between gravity-induced stresses and the material yield stress dictates the success of the mold filling and the production of an adequate void-free monolithic concrete element [1].

The understanding of shaping processes in the standard concrete industry is, in theory, crucial for two reasons. The first one is the optimization of the process itself. For standard concrete casting processes, this may, for instance, take the form of the optimization of pouring points locations [2] or form pressure prediction [3]. The second reason is that only process understanding provides an engineer with the ability to define some target rheological requirements for the fresh material. Fluidity, like mechanical strength, has a technical and economic cost. Being able to define some minimal (or maximal) required values for a given

object geometry and process is therefore critical. In practice, however, processing techniques in the concrete industry do not vary much. Standards and experienced workers at the building site or in a factory are therefore often enough to get a rough but sufficient insight on the fresh properties requirement for a given application. Numerical simulations of fresh concrete flows and processing techniques have therefore been used in the past only for extremely specific (often research-based) cases or in the field of litigations, in which they allow for the *a-posteriori* assessment of the respective responsibilities of the actors involved in a given concrete processing activity.

However, the recent wave of new concrete digital processing techniques, including extrusion-based additive manufacturing, has increased the diversity of the processing technologies available. The industry is therefore facing new shaping techniques that have to be optimized and that impose the use of materials, for which fresh properties requirements are yet to be defined. Within this new frame, it becomes necessary to understand and optimize these processes without the decades of experience associated to standard form filling. However, these new shaping techniques give access to a freedom of shape that results in complex mechanical stress fields, induced by such complex geometries. This prevents most analytical approaches from being able to provide detailed insights, except in the case of the simplest geometries such as basic walls or cylindrical columns [63, 80, 86].

Within this frame, it is the opinion of the present authors that the industrial integration of these shaping techniques may be facilitated by the use of numerical simulations of concrete flow. The numerical simulations may replace (or least reduce) the tedious trials and errors optimization of digital processing technologies. These techniques may moreover allow for the definition of the rheological requirements of the material that is expected to be shaped.

In the first part of this paper, we present the state of the art in the field of numerical simulations of concrete flow from the various numerical techniques available up to some examples of their applications to some standard processes. In the second part of this paper, we focus on the existing literature on numerical simulations of extrusion-based additive manufacturing processes for concrete. We study both the scale of the extruded filament and of the object being printed. We show and emphasize the type of information that can be retrieved from such numerical studies and their practical consequences.

2. *Numerical simulations of concrete flow*

2.1. The various numerical techniques

Partial differential equations (PDE) are used to describe flow behaviour of fluid continuum. Such PDE are often too complex to be solved by analytical means and are thus only solvable with computers. Computers cannot however solve a PDE directly but, as these machines can conduct basic arithmetic operations, they can solve systems of algebraic equations (SAE). Thus, to numerically solve fluid flow with a computer, one must first convert the corresponding PDE over to SAE. Examples of such techniques are the Finite Element Method (FEM), Finite Difference Method (FDM) and the Finite Volume Method (FVM). Regardless of the method used, a group of points in space must be defined, where key variables are calculated. Each element inside a SAE corresponds to such a grid point and the spatial rearrangement of all these points is referred to as the mesh.

In general, one can classify flow simulation techniques into two fundamental groups, the meshless (also known as meshfree or grid-free) methods and the mesh-based methods. As previously mentioned then for the latter, the key variables are solved on a pre-arranged mesh, for example through the FDM [4,5] or by the Lattice-Boltzmann Method (LBM) [5-7]. However, for the meshfree approaches, no specific reference is made to a mesh, but rather each (Lagrangian) particle of the system carries its own physical parameters such as velocity and position [8]. Examples of such method are the well-known Discrete (or Distinct) Element Method (DEM) [5, 9, 10], the Smoothed Particle Hydrodynamics (SPH) [11] and the Dissipative Particle Dynamics (DPD) [5, 6, 11, 12]. Some numerical techniques may locate at the boundary between the two groups (*i.e.* between mesh-based and meshless). For example, recently a meshless version of the LBM has been introduced [13].

The term “Computational Fluid Dynamics” or CFD, refers to approximate solution of the fluid equations in fluid continuum. Solutions can be both based on meshless and mesh-based methods. However, often, the term CFD, is attributed to mesh-based methods only. This becomes apparent when reviewing textbooks about topics such as FDM, FEM or FVM [4, 5, 14-16]. Sometimes, the term “continuous approach” has also been used in relation to such methods [17]. Nonetheless, it should be noted that, in some literature, the term CFD encompasses both the meshless and mesh-based methods [6, 8]. Here, we adopt the terminology from [5] and attribute the term CFD to mesh-based methods only, while acknowledging that this term can in fact have a broader meaning.

Initially, FEM was the most popular choice for the simulation of fresh cement-based materials and early references can be found in [18-20]. Later, FVM started to become more popular, a consequence of it becoming central to the most well-established CFD codes such as CFX/ANSYS, FLUENT, PHOENICS, STAR-CD, Flow-3D and OpenFOAM [16, 21-23]. The use of FVM for the simulation of the fresh cementitious material can for instance be found in [24-30]. There are relatively few instances of FDM simulations of cement-based materials but examples can still be found in [31-33]. One of the reasons for its unpopularity lies in its inability to use unstructured mesh. But such mesh type is necessary for meshing towards and around complex geometries in Cartesian coordinates [16]. For structured mesh, the position of any grid point is uniquely identified by the coordinate system, e.g. x,y,z, and consequently each neighbour cell differs by these indices, e.g. +/- dx,dy,dz [16,17a]. Such neighbour connectivity simplifies programming and the matrix of the SAE has a regular diagonal structure [17a]. However, for the pre-mentioned unstructured mesh, the grid points do not have a reference to the coordinate system, but rather to a label system (each point or cell has a unique label, like an integer number), which is arbitrarily structured [17a]. This allows for a certain freedom in mesh geometry, like no restriction in number of neighbour cells and mixture of different cell types within the same mesh (polyhedral, hexahedra, tetrahedral, etc.). However, the matrix of the corresponding SAE does not have regular diagonal structure and in order to reduce its bandwidth, the cells labels must be reordered.

With the progress of time, more and more simulations of the fresh cement-based materials have been based on meshless approaches. The most popular type is DEM, which is most apparent by the fact that this method was the topic of a whole chapter in the recently published RILEM state-of-the art report [5]. Other advanced meshless methods have also been used when treating the cementitious material like the DPD [12, 17], which is also discussed in [5] along with other newer cutting-edge methods.

In principle, for geometries with dimensions far larger than the size of the constitutive meshless particles, mesh-based and meshless approaches should produce the same/similar results and such an example is shown in Fig. 1. This figure gathers the results of a concrete channel benchmark flow case, where both mesh-based as well as meshless methods were applied [34] and clearly shows that all methods provide results similar to the analytical solution of the problem [34].

2.2. Simulations of tests and rheometers

Rheological properties are either measured using rheometers of various types or industrial tests. To better understand the flow within these devices and thus make a better interpretation of the experimental data, numerical simulations of rheometers and industrial tests have been frequently carried out. One of the earliest attempts to simulate slump test was, for instance, done by Tanigawa and Mori [35].

Different types of rheometers exist, in which many are summarized in [36]. Examples of devices that are designed to provide the user with fundamental physical quantities are the BTRHEOM and the BML rheometer [36]. The former is based on the principle of parallel plates, while the latter is based on the coaxial cylinders system. Simulation results for the BTRHEOM have been obtained both with FEM as well as FDM in [37, 38], while the simulations of the BML have been made based on the FDM in [31, 32]. In both cases, simulations were done to verify and/or analyze the devices in question, as well as enhance interpretations of the experimental data that these tools provide.

One can think of the slump device and the rotational rheometers (i.e. BTRHEOM, BML, etc.) as two endpoint extremes of the range of rheological devices available. In between those two extremities, are devices like the J-Ring test, L-Box, LCPC-box, V-funnel, Orimet and so forth [39, 40]. Many of these have gone through extensive simulation analysis and perhaps the best example of this is the treatment of the L-Box. It has been simulated both with mesh-based methods [28, 41, 42] as well as meshless methods [5, 43, 44]. Other devices like the LCPC-box [34] (see also Figure 1), or the V-funnel have been simulated with both mesh-based and meshless methods [45, 46].

In general (however, with exceptions), for a given rheological device, the computational analysis is initially made with mesh-based methods like the FEM or FDM. Roughly a decade or so after this, the same device is analyzed with meshless methods like the DEM, and, roughly a decade after that, analyzed with more advanced method like the DPD. One of the reasons for this particular time delay, is the increasing computational cost from one method to the next along with the increasing availability of faster computers resources.

Today, the development of new rheological devices is often accompanied by some sort of computational analysis for better understanding of performance and improved results interpretation. For example, Nerella *et al.* [47] recently studied the flow field in the SLIPER rheometer using the software ANSYS Fluent (with the FVM). Also, new simulations have been

applied to older existing equipment, which have previously been too complex to analyze even with mesh-based methods. For example, in [48], series of numerical simulations were made with a supercomputer, to investigate the possibility of using a concrete mixing truck as a rheometer, using FVM. Fig. 2 shows local energy dissipation in W/m^3.

2.3. Simulations of standard castings

Just as numerical simulations in structural mechanics allow civil engineers to identify minimum mechanical properties for reinforced concrete, CFD of casting processes can allow for the specification of required rheological parameters in order to ensure the proper filling of a given formwork [49]. For example, early on, Mori and Tanigawa demonstrated the applicability of Viscoplastic Divided Element Method (VDEM) to simulate the flow of concrete in a reinforced beam section and the filling of a reinforced wall [49] and Kitaoji *et al*. [50] confirmed the applicability of 2D VDEM to simulate the flow of fresh concrete cast into an un-reinforced wall. Numerical simulations were also applied to an industrial casting of a high strength concrete pre-cambered composite beam [51]. The results of the simulations carried out for various values of the rheological parameters, helped to determine the rheological values needed to cast the element [51].

Simulations of large-scale castings are today mostly made with mesh-based methods such as FVM or FDM due to their computational efficiency. Consequently, the current section does not contain any text about usage of meshless methods.

For the mesh-based methods, it is important to be able to divide the flow between the atmospheric air and the fresh concrete. This is usually done with a so-called free interface approach (also called open boundary or moving boundary). Numerical methods that can manage such are classified into two groups depending on the fundamental type of mesh used [52]. These are moving mesh (Lagrangian mesh) and fixed mesh (Eulerian mesh). Although the moving mesh approach allows for a sharp interface definition, they encounter serious problems in cases when the interface undergoes large deformations where the moving mesh may become severely distorted [53]. Because of this, the Eulerian mesh approach is preferred in many cases, like in the volume-of-fluid method [54], the level-set method [53,55] or the marker-and-cell method [55].

Most often, the free interface is treated with the pre-mentioned volume-of-fluid method (VOF) and thus the text that now follows is relative to that specific theory. The free interface

(here, the boundary between the atmospheric air and fresh concrete) is moved through a fixed mesh and is captured by a phase transport equation. Relative to this specific equation, the VOF can be divided between two families, namely the direct methods and the reconstruction methods [56-59].

Unlike geometric interface reconstruction methods, the direct methods do not introduce geometrical representation of the interface, but rather try to maintain a sharply defined interface using properly chosen discretization scheme, commonly known as compressive differencing scheme. Usage of a direct method for the free interface in simulating the flow of fresh concrete in mold/formwork is, for example, available in [60-62]. Fig. 3 shows examples of simulation results made by this approach applied to a whole wall section, length 10 m, thickness 30 cm and height 3.4 m [17]. This particular case also includes the calculation of inhomogeneous aggregate distribution.

3. Numerical simulations of extrusion-based additive manufacturing

3.1. At the scale of the filament

Being able to predict the exact shape of the filament as a function of the fresh material properties and extrusion parameters is a key need for concrete printing. First, most concrete printers are driven by slicing software, which assumes that the extruded filament adopts a theoretical cross-section, resulting from mass conservation and a cross-sectional filament thickness equal to the gap between the nozzle and substrate.

However, a slight difference between this theoretical thickness and the real one can accumulate over a number of layers and thereby substantially alter the cross-section of the subsequently printed filaments. Such cumulated (cross-sectional) deviations can also lead to geometrical unconformities at the scale of the printed concrete component and, in the worst-case scenario, to printing failures. On the other hand, the shape of the filament may also deviate from the expected one when filaments tear, crack or bend in the direction of the deposition (i.e. longitudinal defaults). We will focus below on the numerical prediction of these two kinds of challenges.

In extrusion based additive manufacturing of cementitious materials, two asymptotic regimes have been defined at the level of the nozzle [63], see Fig. 4. Any real extrusion-based additive manufacturing process is expected to be somewhere between these two regimes.

In the first so-called “infinite brick extrusion” regime (Fig. 4 (left)), the cement-based material has a high yield stress compared to gravity-induced stresses and/or stresses resulting from pumping pressure and is unsheared when extruded. As such, the layer leaves the nozzle as a stiff filament, the geometry of which is expected to be the one of the nozzle opening.

In the second regime, Fig. 4 (right), or so-called “free-flow deposition” regime, the material is fully sheared before extrusion either because a low material yield stress or because of a local contraction or a local screw mixer [64]. In this regime, the final geometry of the layer is expected to result from the competition between gravity and yield stress.

For the two first regimes above, it has to be kept in mind that, if the distance between the nozzle and the previous layer is smaller than the nozzle opening, the material is theoretically expected to be locally compressed and deformed until the filament thickness equals the distance between the nozzle and the previous layer. In such a situation, a local over-shoot pressure is however expected to act on the layers below and may further deform the layer or threaten the overall stability of the object being printed.

Finally, for both regimes, when performed at nominal speed (i.e. when extrusion flow rate is equal to the product of the nozzle displacement velocity and the expected cross-section of the filament), a constant and well-controlled filament dimension is expected to be obtained. It is however accepted that, when deviating too far from nominal speed, the extruded filament is prone to either buckling or tearing [65]. Indeed, when the flow rate is higher than the nominal flow rate, some compression stresses do appear inside the filament in the zone between the nozzle exit point and the deposition surface. Depending on the elastic properties of the material being printed and on the free length of the filament, these compressive stresses may induce a localized buckling of the filament. Inversely, a flow rate higher than the nominal one is at the origin of some tensile stress that may, in turn, be at the origin of some cracking.

Both longitudinal (tearing and buckling) and cross-sectional deviations have been modeled in literature. However, despite the above obvious importance of filament shape control and prediction, as of now, only a few numerical studies of additive manufacturing on concrete at the scale of the filament are available in literature. We will review them first below. Then, we will review numerical studies carried out on polymers and put them into a concrete extrusion and deposition perspective.

In Fig. 5, a sketch of a numerical simulation of concrete extrusion is shown [66]. In this model, the printing is simulated by a moving nozzle but a similar result shall be obtained by applying a velocity boundary on the substrate where the material is deposited. The results of the sketched numerical model are presented in Fig. 6 [66]. The plotted cross-section of the printed filaments illustrates that non-Newtonian fluids deposition results into thicker filaments than the reference Newtonian fluid, which itself results into a thicker filament than the theoretical cross-section used by a typical slicing software.

In Fig. 7, a Particle Finite Element Method based numerical model is used to simulate three additively manufacture layers of concrete [67]. The PFEM is a mesh-based approach that solves the governing equations in an updated Lagrangian framework. The numerical model approximates the constitutive law of a Bingham material with a Perzyna formulation, which enables to account for the elastic regime before yielding. The results illustrate that the cross-section of a printed layer is depending on the shape of the previously printed layers. Moreover, the sheer weight of the last printed layer may affect the cross-section of previously printed layers when the stress state exceeds the yield stress of the material (see next section for more details on stability). Thus, this type of numerical simulation can provide very detailed information about cross-sectional shapes that potentially can be incorporated in the slicer software but can also be used, for instance, to predict buildability (see section 2.2.). Simulations of multi-layer prints such as the one seen in Fig. 7 can also be used to quantify the surface roughness quality as well as to design potential tooling and smoothing systems. They also provide a basis for the prediction of contact surface between successive layers, which is a critical feature in interlayer bonding.

In a recent numerical study [65], the influence of variations in process parameters (robot speed and extrusion rate), geometrical features of the filament and nozzle (size and deposition height), as well as material properties (elastic stiffness, yield stress, and viscosity), was systematically explored by means of Finite Volume Method (FVM) numerical modelling, with a reconstruction based VOF approach (Cf. previous section). It was shown that, for a process performed at nominal speed, the cross section of the filament is constant and no variations in stress distributions are present. When the process settings deviate, so that the extrusion rate is higher than the robot speed, filament buckling occurs, illustrated in Fig. 8 (left). An increment in deposition height, as well as an increase in material properties such as stiffness, yield stress and viscosity, were all found to enhance the geometric buckling occurrence as well

as stress inhomogeneity. On the contrary, for an extrusion rate lower than the robot speed, filament tearing occurs, illustrated in Fig 8 (right). A reduction of the material critical strain (*i.e.* the maximal strain that the material can withstand before yielding) was found to have a profound effect on the occurrence of filament tearing [65].

In the case of extrusion-based additive manufacturing of polymers, Fig. 9 presents a comparison between experimental and numerical results for different gaps between the nozzle and substrate [68]. This study showed that a numerical model that treats the material as Newtonian can capture the first order effects in polymer printing, because it is a creeping flow and the polymer solidifies very quickly after deposition. A similar study would be of great importance for simulation of concrete printing in order to identify the appropriate constitutive law (*e.g.* a visco-plastic or elasto-visco-plastic model) that provides a good agreement between model and experiment. This would be specifically relevant for free flow deposition. Numerical models have also been used to detect under- and overfill regimes when printing corners with polymers that are simulated in a similar fashion as previously mentioned (*i.e.* Newtonian), see Fig. 10. Printing sharp corners is a non-trivial task and most additively manufactured concrete structures are produced with rounded shapes and corners. However, simulation tools can be applied to find the ideal nozzle geometry and deposition strategy for a given corner. In this regard, one of the strengths of numerical models is that they can test a wide range of scenarios in a time- and cost-efficient manner, as several simulations can be executed simultaneously.

In Fig. 11, experimental and simulation results of printed structures on a meso-scale are shown. These meso-structures are obtained by deposition of multiple strands of polymer forming a representative volume element for a given printing strategy. The results illustrate the fact that numerical models are able of capturing the trends in the physical prints with a quite good agreement. Based on the predicted meso-structures, porosities can be detected, minimized or controlled with the right printing strategy. A similar approach may also benefit the quality of inter- and intra-layer bond lines in concrete printing.

3.2. At the scale of the printed element

In extrusion based additive manufacturing processes, gravity-induced stresses in the printed element increase as successive layers of fresh cementitious materials are deposited. In the absence of confinement by (traditional) formwork, this gradual increase may lead to structural

failure of a printed element during manufacturing. Two failure mechanisms have been distinguished: *elastic buckling* and *plastic collapse* [63, 71, 72], see Fig. 12. Elastic buckling relates to failure induced by a loss of geometrical stability, while plastic collapse indicates that the material yield stress has been reached.

The occurrence and type of failure is strongly dependent on the object geometry, the material properties, as well as the process parameters. For instance, exceeding the yield stress due to self-weight typically occurs in the bottom of a straight wall, but this location may be less straightforward to define for complex geometries, multi-material printing, or when process parameters are not constant over the object height. Even if failure does not occur, the elastic deformations due to successive layers should be controlled, as not to compromise the geometric conformity of the final product. For such complex process and product dependency, numerical simulations provide valuable insight. Where the *visco-plastic* behavior is the basis of numerical simulations of an individual filament (see previous section), for numerical analyses at the scale of a printed element, the *elastic-plastic* behavior of the early age material, and its structuration kinetics, are critical [73-75]

The elastic material behavior, required both to derive the elastic deformations as well as to assess failure by elastic buckling, may be captured by defining the elastic stiffness (or Young's modulus) and the Poisson's ratio. Plasticity can be analyzed by defining the yield stress of the material. As the thixotropic cementitious materials are at rest for the majority of the printing process, both elastic and plastic material properties are not constant within the time frame of manufacturing, but rather evolve as a function of material age, typically expressed through a structuration rate A_{thix} [76], which may follow both a linear and non-linear trend [77].

To define numerical simulations input, such as elastic and plastic material properties and their rate of structuration, various researchers have proposed experimental methods that move away from what is commonly considered for fresh cementitious materials, and have instead adopted methods based on soil tests or mechanical testing of hardened concrete. Variations around several standard mechanical and rheological tests have been proposed to assess material input parameters in the time frame of typical additive manufacturing processes [71, 78-82, 86]. In addition to these mechanical properties, numerical models of the printing process should incorporate the growing geometry and corresponding increment of gravity induced stresses, as well as printing process parameters such as printing speed, contour length, and thus, object growth rate.

The parametric model proposed by Suiker [72] allows for a rapid pre-simulation evaluation of structural failure in 3D printed wall structures. It was demonstrated that the relatively large number of parameters involved in 3D concrete printing processes may be reduced to five unique dimensionless parameters. Three of these relate to the occurrence of elastic buckling while the two others relate to plastic collapse. Based on this numerical approach, numerous design graphs were constructed which may be utilized to quickly establish the object failure height and the transition point from elastic buckling towards plastic collapse, for variations in process parameters, geometry and boundary conditions, as well as rate of structuration.

The numerical model developed in [71] allows for the analysis of any complex 3D printed geometry. This model is based on the Finite Element Method (FEM). A geometrical non-linear analysis of the printing process is performed, where layers (and thus additional gravity loading), are added stepwise during the analysis, see Fig. 13. The speed of activation follows from the process parameters and contour length, and the elastic and plastic material properties develop correspondingly throughout the analysis. As such, the influence of variations in geometry, material behavior, or process parameters can be studied systematically using dedicated FEM simulations.

The numerical results of both models [71, 72] were validated against printing trials of linear wall structures with various contour lengths. The moment and type of failure was captured by high-resolution photography. From these studies, it was concluded that numerical models are able to predict the failure-deformation accurately, as well as the critical height at which failure occurs for relatively small objects. For larger objects and/or longer printing processes, the accuracy of the numerical predictions drops. This was attributed to the influence of thermal heating of the 3D printer setup over long printing processes, which was not yet incorporated in the experimental characterization nor numerical analyses [83]. These findings stimulate the development towards numerical modelling of the 3D printing process including thermal and moisture effects, which will further increase their accuracy. Such extensions may moreover provide a basis for the numerical assessment of the bond strength between successive layers, which was shown to be likewise dependent on material age and the environmental conditions of the printing process [84, 85].

4. CONCLUSIONS

In the first part of this paper, we presented the state of the art in the field of numerical simulations of concrete flow from the various numerical techniques available up to some examples of their applications to some standard processes. In the second part of this paper, we focused on the existing literature on numerical simulations of extrusion-based additive manufacturing processes for concrete. We studied both the scale of the extruded filament and of the object being printed. Our review shows that numerical modelling tools of extrusion-based additive manufacturing are able to detect and predict the occurrence and type of structural failures through the printing process, no matter if these happen at the scale of the nozzle, at the scale of one layer or at the scale of the entire object being printed. As they allow for a systematic evaluation of the influence of the entire range of material, geometric and process parameters, numerical modelling can be considered as being available to optimize printing quality and material usage.

5. References

[1] Roussel, N., Rheology of fresh concrete: from measurements to predictions of casting processes, Materials and Structures, 40(10), pp. 1001-1012, 2007.

[2] Roussel, N., Staquet, S., Schwarzentruber, L.D., Le Roy, R., Toutlemonde, F., SCC casting prediction for the realization of prototype VHPC-precambered composite beams, MATERIALS AND STRUCTURES, Volume: 40 Issue: 9 Pages: 877-887, 2007

[3] Ovarlez, G. ; Roussel, N, A physical model for the prediction of lateral stress exerted by self-compacting concrete on formwork, Materials and Structures, 39(2), pp. 269-279, 2006.

[4] J. D. Anderson. Computational Fluid Dynamics, The Basics with Applications. McGraw-Hill, Inc., USA, 1995.

[5] N. Roussel, A. Gram (Eds.), Simulation of Fresh Concrete Flow, State-of-the Art Report of the RILEM Technical Committee 222-SCF, Springer 2014.

[6] J. Tu, G. Heng, Y.C. Liu, Computational Fluid Dynamics - A Practical Approach, Butterworth-Heinemann, 2008.

[7] O. Svec, J. Skocek, H. Stang, M.R. Geiker, N. Roussel, Free surface flow of a suspension of rigid particles in a non-Newtonian fluid: a lattice Boltzmann approach, J. Non-Newtonian Fluid Mech. 179-180 (2012) 32-42.

[8] K. Stefan, R. Gunther, CFD-Simulations In The Early Product Development, Procedia CIRP 40 (2016) 443-448.

[9] V. Mechtcherine, A. Gram, K. Krenzer, J-H. Schwabe, S. Shyshko, N. Roussel, Simulation of fresh concrete flow using Discrete Element Method (DEM): Theory and applications, Mater. Struct. 47 (2014) 615-630.

[10] C. O'Sullivan, Particulate discrete element modelling - A Geomechanics perspective, Spon Press, USA, 2011.

[11] Pep Espanol, Patrick Warren, Perspective: Dissipative particle dynamics, J. Chem. Phys. 146, (2017) 150901:1-16.

[12] N.S. Martys, Study of a dissipative particle dynamics based approach for modeling suspensions, J. Rheol. 49 (2005) 401-424.

[13] S.H. Musavi, M. Ashrafizaadeh, A mesh-free lattice Boltzmann solver for flows in complex geometries, Int. J. Heat Fluid Flow 59 (2016) 10-19.

[14] O. Zikanov, Essential Computational Fluid Dynamics, John Wiley & Sons, Inc., USA, 2010.

[15] C. A. J. Fletcher, Computational Techniques for Fluid Dynamics, volume I. Springer Series in Computational Physics, Springer-Verlag, Germany, 2nd edition, 1990.

[16] H.K. Versteeg, W. Malalasekera, An Introduction to Computational Fluid Dynamics-The Finite Volume Method (2nd ed), Pearson Education Limited, England, 2007.

[17a] J.H. Ferziger, M. Peric, Computational Methods for Fluid Dynamics (3rd ed), Springer-Verlag, 2002.

[17] K. Vasilic, A. Gram, J.E. Wallevik, Numerical simulation of fresh concrete flow: insight and challenges, RILEM Technical Letters, 4 (2019) 57-66.

[18] H. Mori, Y. Tanigawa, Simulation methods for fluidity of fresh concrete, Memoirs of the School of Engineering, vol. 44, pp. 71-133, Nagoya University, 1992.

[19] Y. Kurokawa, Y. Tanigawa, H. Mori, Y. Nishinosono, Analytical study on effect of volume fraction of coarse aggregate on Bingham's constants of fresh concrete, Transactions of the Japan Concrete Institute 18 (1996) 37-44.

[20] G. Christensen, Modelling the flow of fresh concrete: The slump test, PhD thesis, Princeton University, 1991.

[21] A. Gharehbaghi, B. Kaya and H. Saadatnejadgharahassanlou, Numerical simulation of two dimensional unsteady flow by total variation diminishing scheme, International Journal of Engineering & Applied Sciences (IJEAS), 8(3) (2016) 1-14.

[22] H.G. Weller, Derivation modelling and solution of the conditionally averaged two-phase flow equations, Technical Report TR/HGW/02, Nabla Ltd. 2002.

[23] H. Rusche, Computational Fluid Dynamics of Dispersed Two-Phase Flows at High Phase Fractions, Ph.D. thesis, Department of Mechanical Engineering, Imperial College of Science, Technology & Medicine, London, 2002.

[24] N. Roussel, P. Coussot, “Fifty-cent rheometer” for yield stress measurements: from slump to spreading flow, J. Rheol. 49(3) (2005) 705-718.

[25] L.N. Thrane, P. Szabo, M. Geiker, M. Glavind, H. Stang, Simulation and verification of flow in SCC test methods. Proc. of the 4th Int. RILEM Symp. on SCC, 2005, Chicago.

[26] N. Roussel, Correlation between yield stress and slump: Comparison between numerical simulations and concrete rheometers results, Mater. Struct. 39(4) (2006) 501-509.

[27] L.N. Thrane, Form-filling with Self-Compacting Concrete, Ph-D Thesis, Danish Technological Institute, Technical University of Denmark, Lyngby, 2007.

[28] A. Gram, Modelling Bingham Suspensional Flow, PhD thesis, KTH Royal Institute of Technology, Sweden, 2015.

[29] J. Spangenberg, N. Roussel, J.H. Hattel, H. Stang, J. Skocek, M.R. Geiker, Flow induced particle migration in fresh concrete: theoretical frame, numerical simulations and experimental results on model fluids, Cem. Concr. Res. 42 (2012) 633-641.

[30] K. Vasilic, W. Schmidt, H.C. Kuhne, F. Haamkens, V. Mechtcherine, N. Roussel, Flow of fresh concrete through reinforced elements: experimental validation of the porous analogy numerical method, Cem. Concr. Res. 88 (2016) 1-6.

[31] J.E. Wallevik, Minimizing end-effects in the coaxial cylinders viscometer: Viscoplastic flow inside the ConTec BML Viscometer 3, J. Non-Newtonian Fluid Mech. 155(3) (2008) 116-123.

[32] J.E. Wallevik, Rheology of Particle Suspensions - Fresh Concrete, Mortar and Cement Paste With Various Types of Lignosulfonates, Dr.ing. thesis, Department of Structural Engineering, The Norwegian University of Science and Technology, Norway, 2003, http://ntnu.diva-portal.org

[33] D. Feys, J.E. Wallevik, A. Yahia, K.H. Khayat, O.H. Wallevik, Extension of the Reiner-Riwlin equation to determine modified Bingham parameters measured in coaxial cylinders rheometers, Mater. Struct. 46 (2013) 289-311.

[34] N. Roussel, A. Gram, M. Cremonesi, L. Ferrara, K. Krenzer, V. Mechtcherine, S. Shyshko, J. Skocec, J. Spangenberg, O. Svec, L.N. Thrane, K. Vasilic, Numerical simulations of concrete flow: A benchmark comparison, Cem. Concr. Res. 79 (2016) 265-271.

[35] Y. Tanigawa, H. Mori, Rheological analysis of slumping behavior of fresh concrete, Proceedings of the 29th Japan congress on materials research 1986.

[36] P. F. G. Banfill, D. Beaupre, F. Chapdelaine, F. de Larrard, P. Domone, L. Nachbaur, T. Sedran, O. H. Wallevik, J. E. Wallevik, Comparison of Concrete Rheometers: International Tests at LCPC (Nantes, France) in October, 2000 (NISTIR 6819), (eds. F. Ferraris, L. E. Brower), National Institute of Standard and Technology (NIST), Gaithersburg, USA, 2001.

[37] C. Hu, Rhéologie des bétons fluides, Ecole Nationale des Ponts et Chaussées, 1995.

[38] C. Hu, F. de Larrard, T. Sedran, C. Boulay, F. Bosc, F. Deflorenne, Validation of BTRHEOM, the new rheometer for soft-to-fluid concrete, Mater. Struct. 29(194) (1996) 620-631.

[39] P.J.M. Bartos, M. Sonebi, A.K. Tamimi (Eds.), Workability and Rheology of Fresh Concrete: Compendium of Tests, Report of RILEM Technical Committee TC 145-WSM, RILEM Publications S.A.R.L., Cachan Cedex, France, 2002.

[40] N. Roussel, The LCPC BOX: a cheap and simple technique for yield stress measurements of SCC, Mater. Struct. 40 (2007) 889-896.

[41] L.N. Thrane, P. Szabo, M.R. Geiker, M. Glavind, H. Stang, Simulation of the test method L-box for self-compacting concrete, Annual Transactions of the Nordic Rheology Society, 12 (2004) 47-54.

[42] M. Cremonesi, L. Ferrara, A. Frangi, U. Perego, Simulation of the flow of fresh cement suspensions by a Lagrangian finite element approach, J. Non-Newtonian Fluid Mech. 165 (2010) 1555-1563.

[43] R. Deeb · S. Kulasegaram · B. L. Karihaloo, 3D modelling of the flow of self-compacting concrete with or without steel fibres. Part II: L-box test and the assessment of fibre reorientation during the flow, Comp. Part. Mech. 1 (2014) 391-408.

[44] M. AL-Rubaye, S. Kulasegaram, B.L. Karihaloo, Simulation of self-compacting concrete in an L-box using smooth particle hydrodynamics, Mag. Concrete Res. 69(12) (2017) 618-628.

[45] K. Vasilic, B. Meng, H.C. Kühne, N. Roussel, Flow of fresh concrete through steel bars: A porous medium analogy, Cement and Concrete Research 41 (2011) pp. 496–503.

[46] H. Lashkarbolouk, A.M. Halabian, M.R. Chamani, Simulation of concrete flow in V-funnel test and the proper range of viscosity and yield stress for SCC, Mater. Struct. 47 (2014) 1729-1743.
[47] V.N. Nerella, V. Mechtcherine, Virtual sliding pipe rheometer for estimating pumpability of concrete, Construction and Building Materials, 170 (2018) 366-377.
[48] J.E. Wallevik, O.H. Wallevik, Concrete mixing truck as a rheometer, Cem. Concr. Res. 127 (2020) 105930.
[49] N. Roussel, M.R. Geiker, F. Dufour, L.N. Thrane, P. Szabo, Computational modeling of concrete flow: General overview, Cem. Concr. Res. 37 (2007) 1298-1307.
[50] H. Kitaoji, Y. Tanigawa, H. Mori, Y. Kurokawa, S. Urano, Flow Simulation of Fresh Concrete Cast into Wall Structure by Viscoplastic Divided Space Element Method, Transactions of the Japan Concrete Institute, 16 (1996) 45-52.
[51] N. Roussel, S. Staquet, L. D'Aloia Schwarzentruber, R. Le Roy, F. Toutlemonde, SCC casting prediction for the realization of prototype VHPC-precambered composite beams, Mater. Struct. 40(9) (2007) 877-887.
[52] D. Gerlach, G. Tomar, G. Biswas, F. Durst, Comparison of volume-of-fluid methods for surface tension-dominant two-phase flows, Int. J. Heat. Mass. Tran. 49 (2006) 740-754.
[53] E. Berberovic, Investigation of Free-surface Flow Associated with Drop Impact: Numerical Simulations and Theoretical Modeling, PhD thesis, Technische Universitat Darmstadt, Darmstadt, 2010.
[54] C.W. Hirt, B.D. Nichols, Volume of fluid (VOF) method for the dynamics of free boundaries, J. Comput. Phys. 39 (1) (1981) 201-225.
[55] V.R. Gopala, B.G.M. van Wachem, Volume of fluid methods for immiscible-fluid and free-surface flows, Chem. Eng. J. 141 (2008) 204-221.
[56] J. Klostermann, K. Schaake, R. Schwarze, Numerical simulation of a single rising bubble by VOF with surface compression, Int. J. Numer. Meth. Fluids 71(8) (2013) 960-982.
[57] D.L. Youngs, An Interface Tracking Method For a 3D Eulerian Hydrodynamics Code, Technical Report AWRE/44/92/35, Atomic Weapons Research Establishment, 1987.
[58] W. Noh, P. Woodward, SLIC (simple line interface calculation), in: Proceedings of the Fifth International Conference on Fluid Dynamics, in: A. Van devooren, P. Zandbergen (Eds.), Lecture Notes in Physics, vol. 59, Springer-Verlag, Berlin, 1976.

[59] J. Spangenberg, Numerical Modelling of Form Filling with Self-Compacting Concrete, Ph.D. thesis, Department of Mechanical Engineering, Technical University of Denmark (DTU), Lyngby, 2012.

[60] J.E. Wallevik, W. Mansour, O.H. Wallevik, Computational Segregation Analysis during Casting of SCC: In K.H. Khayat (Ed.) SCC 2016 8th International RILEM Symposium on Self-Compacting Concrete, Washington DC, USA, 15-18 May 2016.

[61] J.E. Wallevik, W. Mansour, O.H. Wallevik, OpenFOAM casting solver with segregation, International RILEM conference on materials, systems and Structures in Civil Engineering, Conference segment on Fresh Concrete, RILEM Publications S.A.R.L. ISBN: 978-2-35158-184-1, 22-24 August, Technical University of Denmark, Lyngby, Denmark (2016).

[62] J.E. Wallevik, W. Mansour, O.H. Wallevik, Computational Segregation Analysis During Casting of SCC. In: V. Mechtcherine, K.H. Khayat, E. Secrieru (eds) Rheology and Processing of Construction Materials. RheoCon 2019, SCC 2019. RILEM Bookseries, vol 23. Springer, Cham, 2020.

[63] N. Roussel. Rheological requirements for printable concretes. Cement and Concrete Research, 112:76–85, 2018.

[64] V. Mechtcherine at al., Extrusion-based additive manufacturing with cement-based materials – Processing steps and their underlying physics, same special issue.

[65] R.J.M. Wolfs, T.A.M. Salet, N. Roussel. Filament geometry control in extrusion based additive manufacturing. Journal paper in preparation.

[66] R. Comminal, M. P. Serdeczny, N. Ranjbar, M. Mehrali, D. B. Pedersen, H. Stang, J. Spangenberg, 2019, Modelling of material deposition in big area additive manufacturing and 3D concrete printing, Joint Special Interest Group meeting between euspen and ASPE – Advancing Precision in Additive Manufacturing.

[67] J. Reinold, J. J. Timothy, G. Meschke, 2019, Particle finite element simulation for additively manufacturing processes of fresh concrete, Proceedings of the 8th GACM Colloquium on Computational Mechanics for Young Scientists from Academia and Industry, 339-342.

[68] M. P. Serdeczny, R. Comminal, D. B. Pedersen, J. Spangenberg, (2018), Experimental validation of a numerical model for the strand shape in material extrusion additive manufacturing, Additive Manufacturing, 24:145-153.

[69] R. Comminal, M. P. Serdeczny, D. B. Pedersen, J. Spangenberg, 2019, Motion planning and numerical simulation of material deposition at corners in extrusion additive manufacturing, Additive Manufacturing, 29:100753.

[70] M. P. Serdeczny, R. Comminal, D. B. Pedersen, J. Spangenberg, 2019, Numerical simulations of the mesostructure formation in material extrusion additive manufacturing, Additive Manufacturing, 28:419-429.

[71] R. J. M. Wolfs, F. P. Bos, and T. A. M. Salet. Early age mechanical behaviour of 3D printed concrete: Numerical modelling and experimental testing. Cement and Concrete Research, 106:103–116, 2018.

[72] A. S. J. Suiker. Mechanical performance of wall structures in 3D printing processes: Theory, design tools and experiments. International Journal of Mechanical Sciences, 137:145–170, 2018.

[73] N. Roussel, G. Ovarlez, S. Garrault, and C. Brumaud. The origins of thixotropy of fresh cement pastes. Cement and Concrete Research, 41(1):148–157, 2012.

[74] L. Reiter, T. Wangler, N. Roussel, and R. J. Flatt. The role of early age structural build-up in digital fabrication with concrete. Cement and Concrete Research, 112:86–95, 2018.

[75] Roussel, N, Bessaies-Bey, H, Kawashima, S., Marchon; D., Vasilic, K., Wolfs, R., Recent advances on yield stress and elasticity of fresh cement-based materials, Cement and Concrete Research, 2019

[76] N. Roussel. A thixotropy model for fresh fluid concretes: Theory, validation and applications. Cement and Concrete Research, 36(10):1797–1806, 2006.

[77] A. Perrot, A. Pierre, S. Vitaloni, V. Picandet, Prediction of lateral form pressure exerted by concrete at low casting rates, Materials and Structures, 48(7) (2015) pp. 2315-2322.

[78] L. K. Mettler, F. K. Wittel, R. J. Flatt, and H. J. Herrmann. Evolution of strength and failure of SCC during early hydration. Cement and Concrete Research, 89:288–296, 2016.

[79] R. J. M. Wolfs, F. P. Bos, and T. A. M. Salet. Correlation between destructive compression tests and non-destructive ultrasonic measurements on early age 3D printed concrete. Construction and Building Materials, 181:447–454, 2018.

[80] A. Perrot, D. Rangeard, and A. Pierre. Structural built-up of cement-based materials used for 3D-printing extrusion techniques. Materials and Structures, 49(4):1213–1220, 2016.

[81] R. Jayathilakage, J. Sanjayan, P. Rajeev. Direct shear test for the assessment of rheological parameters of concrete for 3D printing applications. Materials and Structures, 52(12), 2019.

[82] R. J. M. Wolfs, F. P. Bos, and T. A. M. Salet. Triaxial compression testing on early age concrete for numerical analysis of 3D concrete printing. Cement and Concrete Composites, 104, 2019.

[83] R. J. M. Wolfs and A. S. J. Suiker. Structural failure during extrusion-based 3D printing processes. Int. Journal of Advanced Manufacturing Technology, 2019

[84] E. Keita, H, Bessaies-Bey, W, Zuo, P. Belin, N. Roussel. Weak bond strength between successive layers in extrusion-based additive manufacturing: measurement and physical origin. Cement and Concrete Research 123 2019

[85] R. J. M. Wolfs, F. P. Bos, and T. A. M. Salet. Hardened properties of 3D printed concrete: The influence of process parameters on interlayer adhesion. Cement and Concrete Research, 119:132–140, 2019.

[86] Jacques Kruger, Seung Cho, Stephan Zeranka, Celeste Viljoen, Gideon van Zijl, 3D concrete printer parameter optimisation for high rate digital construction avoiding plastic collapse, Composites Part B: Engineering, Volume 183, 15 February 2020, 107660

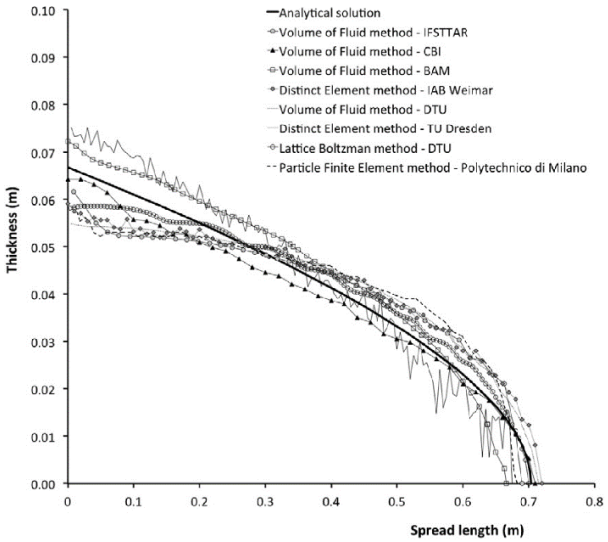

Figure 1. Comparison of the various simulations for the channel flow [34].

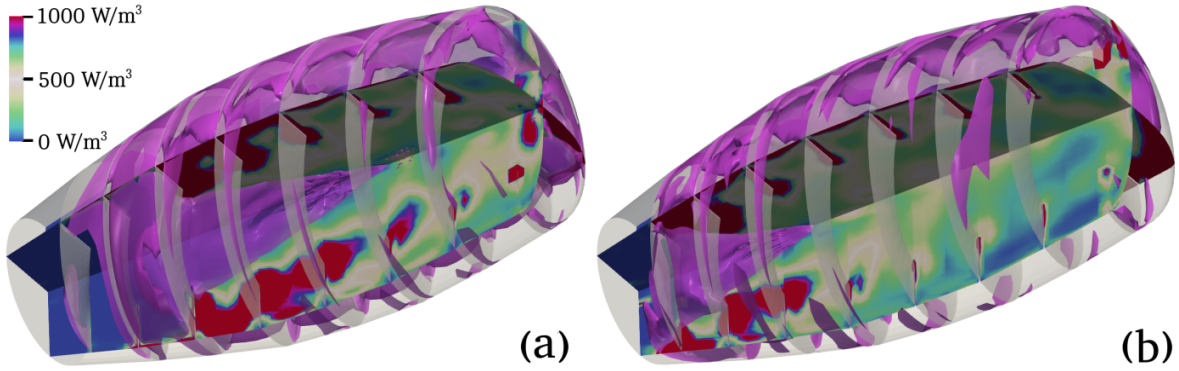

Figure 2. Simulation of concrete flow inside the drum of a concrete mixing truck using FVM [48]. Local energy dissipation is plotted for a drum rotation of 0.19 Rps, with 75 Pa.s for plastic viscosity and zero yield stress. 5.4 m^3 of concrete (Fig. 2a) and 8.2 m^3 of concrete (Fig. 2b)

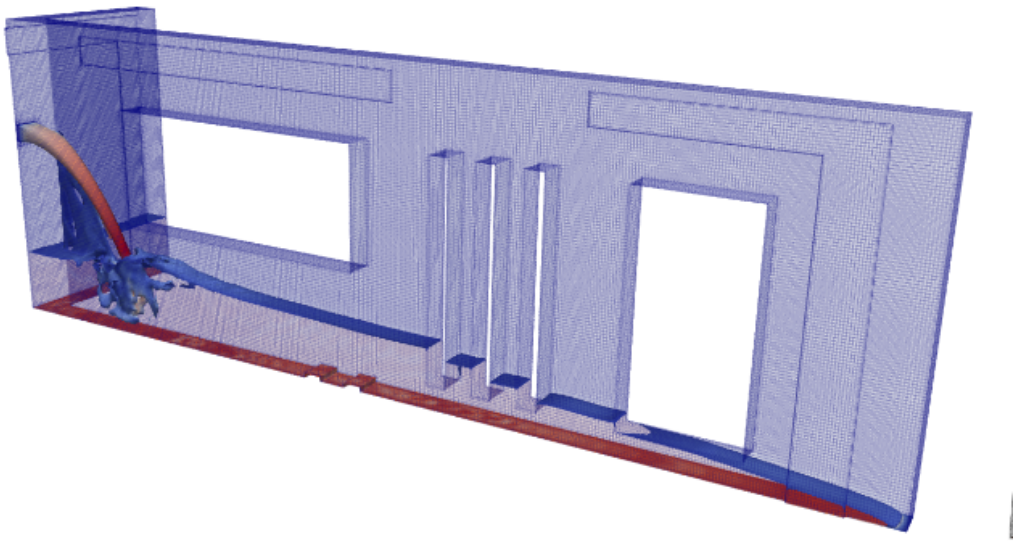

Figure 3. Example of usage of a direct method for the free interface during a large-scale simulation of a wall section casting [17].

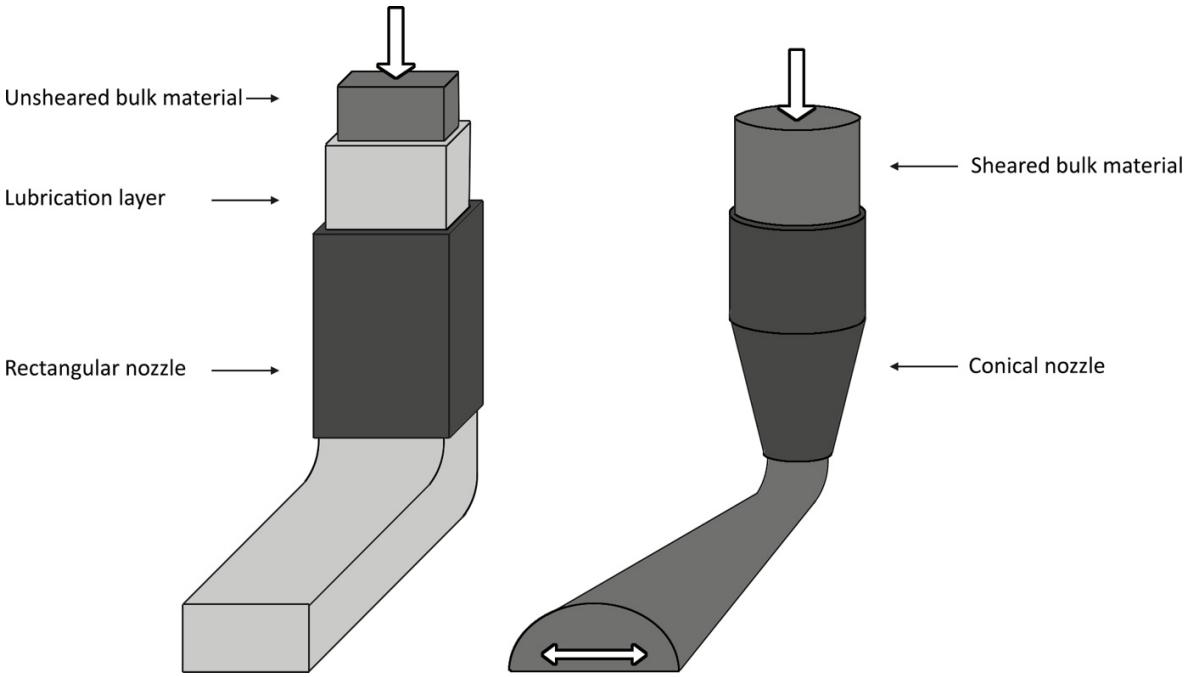

Figure 4. The two asymptotic regimes for concrete extrusion in additive manufacturing. (left) the so-called "infinite brick" regime; (right) the "free flow deposition" regime (extracted from [63].

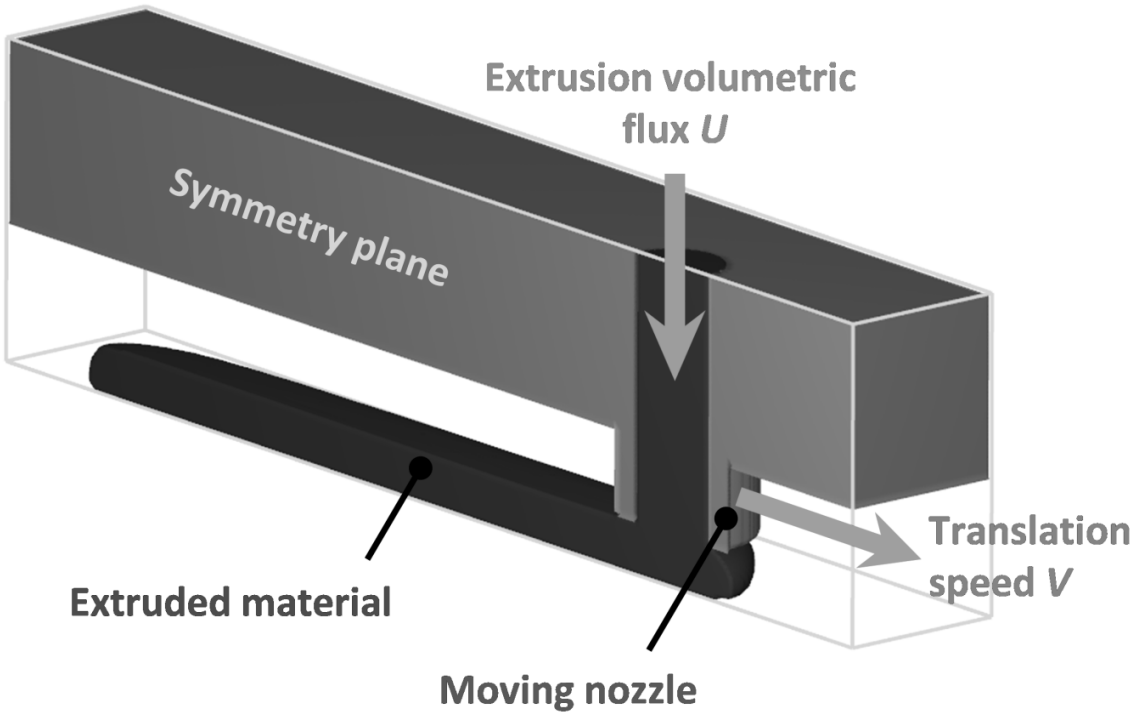

Figure 5. Sketch of the geometry and boundary conditions of a numerical model simulating material extrusion additive manufacturing of concrete [66].

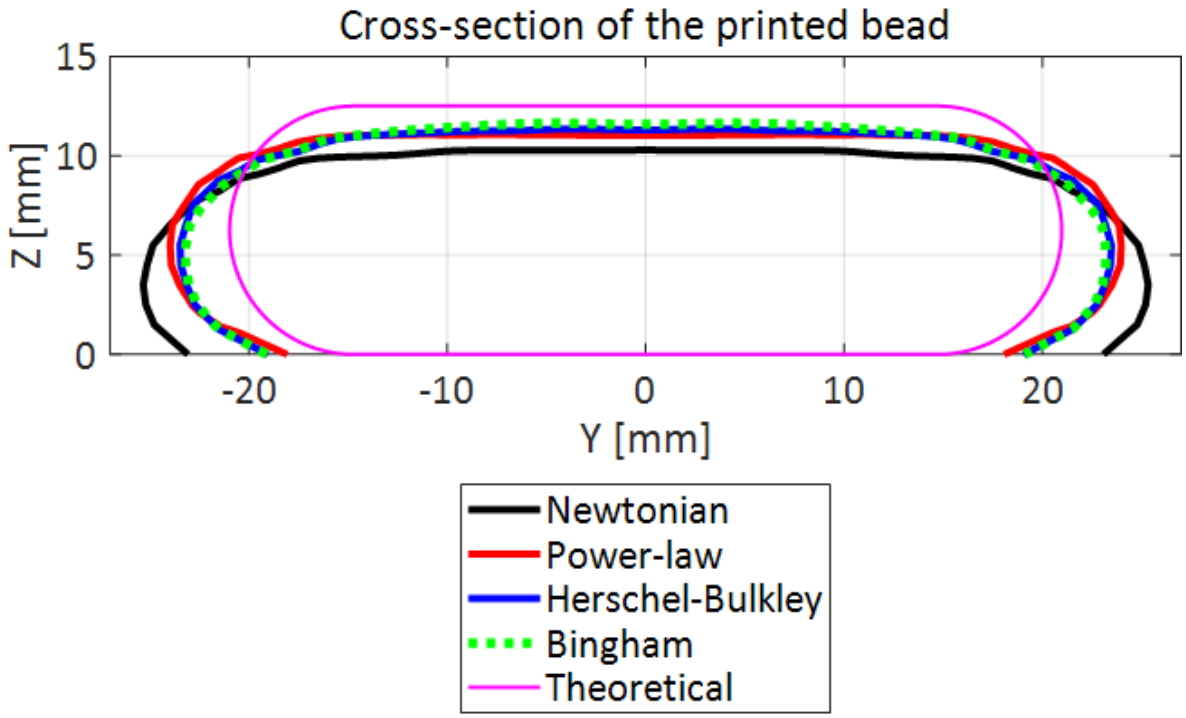

Figure 6. Computational fluid dynamics results of the cross-section of printed strands with different constitutive models [66].

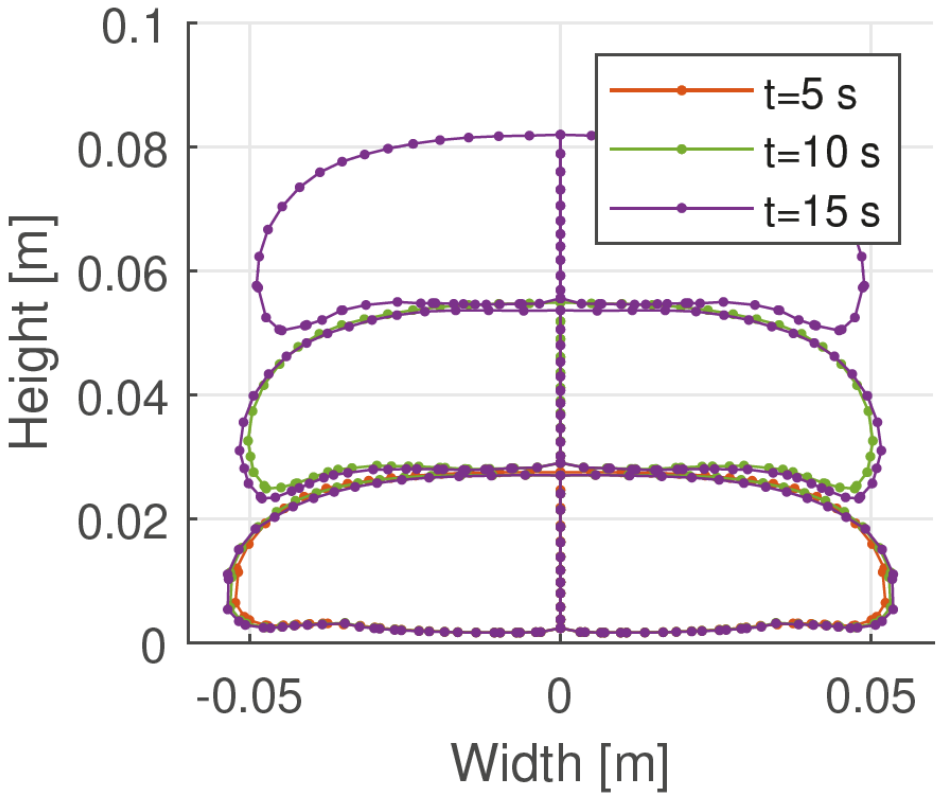

Figure 7. Particle finite element method-based results of the cross-section of three additively manufactured layers using an approximated Bingham material model, reproduced from [67].

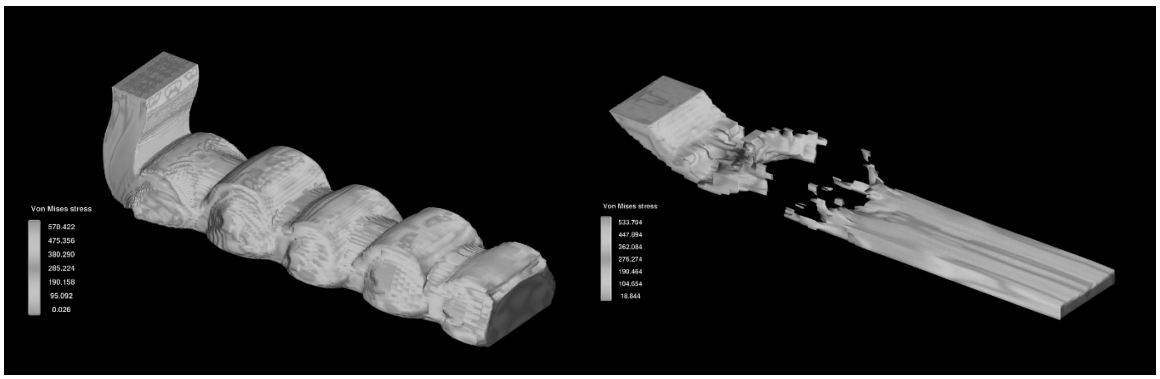

Figure 8. Uncontrolled filament geometry during extrusion: filament buckling (left) and filament tearing (right), obtained by 3D CFD modelling.

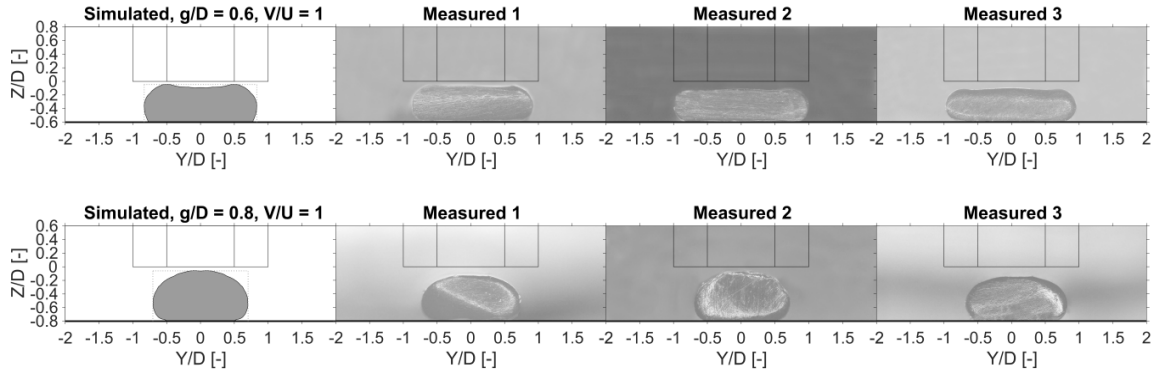

Figure 9. Simulated and experimental cross-sections of strands printed with different gaps between the nozzle and substrate [68].

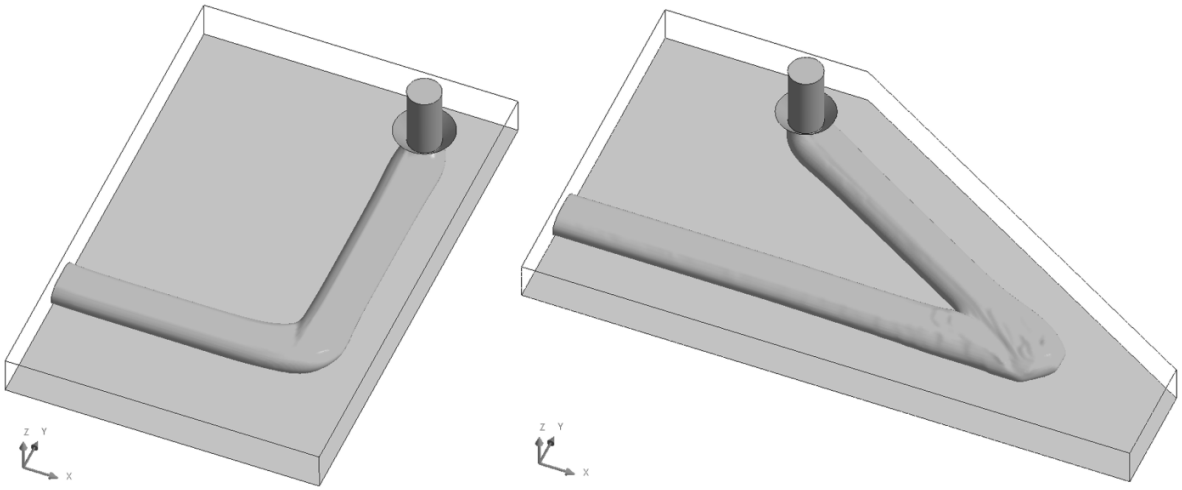

Figure 10. Simulated material deposition for 90˚ and 30˚ corners printing [69].

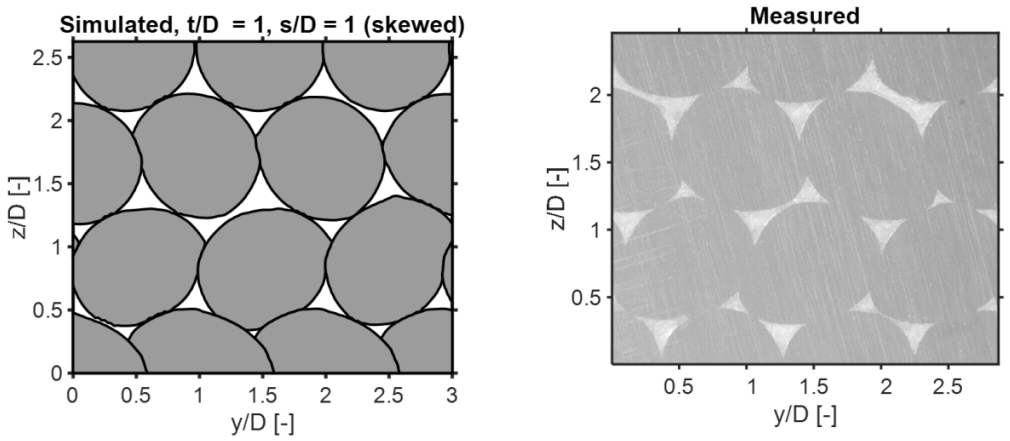

Figure 11. Simulated and experimental meso-structures obtained with a skewed printing strategy [70].

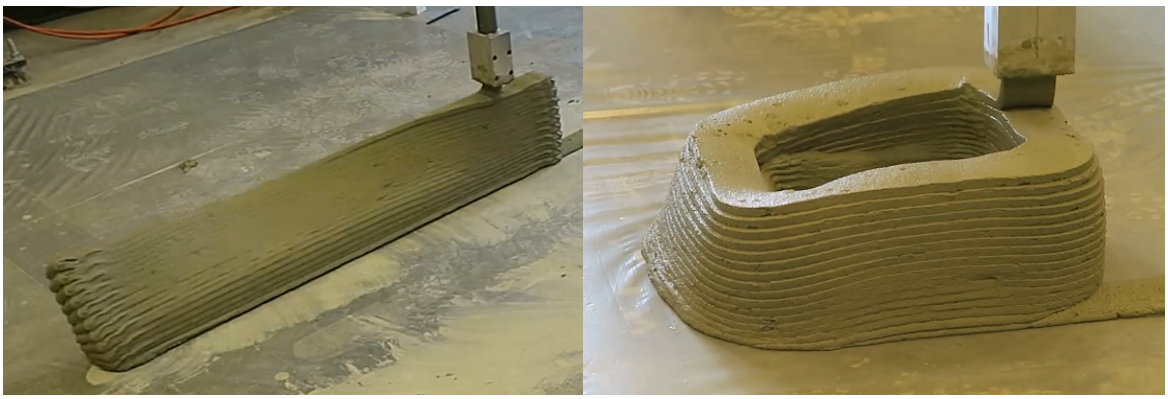

Figure 12. Elastic buckling (left) and plastic collapse (right) observed in printing experiments.

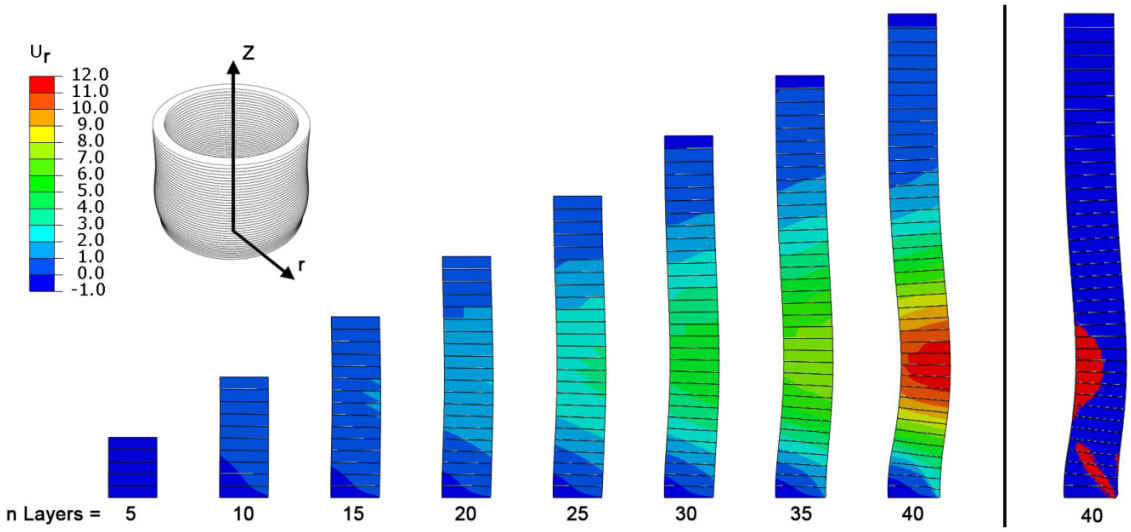

Figure 13. FEM analysis results of the 3D printing process of a cylinder presented at various steps during the printing process.

Declaration of interests

 The authors declare that they have no known competing financial interests or personal relationships that could have appeared to influence the work reported in this paper.

☐The authors declare the following financial interests/personal relationships which may be considered as potential competing interests: